Received: 6 December 2021 | Revised: 9 February 2022 | Accepted: 23 February 2022

DOI: 10.1002/aoc.6661

FULL PAPER

Applied Organometallic Chemistry WILEY

# Synthesis and antiproliferative study of phosphorescent multimetallic Re(I)/Au(I) complexes containing fused imidazo[4,5-f]-1,10-phenanthroline core

**Andrés Luengo**[1] | **Isabel Marzo**[2] | **Vanesa Fernández-Moreira**[1] | **M. Concepción Gimeno**[1]

[1]Departamento de Química Inorgánica, Instituto de Síntesis Química y Catálisis Homogénea (ISQCH), CSIC-Universidad de Zaragoza, Zaragoza, Spain

[2]Departamento de Bioquímica y Biología Molecular, Universidad de Zaragoza, Zaragoza, Spain

**Correspondence**
Vanesa Fernández-Moreira and M. Concepción Gimeno, Departamento de Química Inorgánica, Instituto de Síntesis Química y Catálisis Homogénea (ISQCH), CSIC-Universidad de Zaragoza Pedro Cerbuna 12, 50009, Zaragoza, Spain.
Email: gimeno@unizar.es; vanesa@unizar.es

**Funding information**
Agencia Estatal de Investigación, Grant/Award Numbers: PID2019-104379RB-C21, RED2018-102471-T, RTI2018-097836-J-I00, RYC2018-025872-I; Gobierno de Aragón-Fondo Social Europeo, Grant/Award Number: E07_20R

Five heterobimetallic $Re^{I}/Au^{I}$ and a tri-metallic $Re^{I}/Au^{I}/Re^{I}$ species following the formulas *fac*-[ReCl $(CO)_3$(N^N^CAuR)]$^{0/+}$ and [(*fac*-[ReCl $(CO)_3$(N^N^C)])$_2$Au]$^{+}$, where R is an iodide (**1**), phenylacetylene (**2**), dodecanethiol (**3**), 2,3,4,6-tetra-*O*-acetyl-1-thio-β-D-glucopyranose (**4**) and JohnPhos (**5**) and N^N^C is the fused imidazo[4,5-f]-1,10-phenanthroline heterotopic ligand, were synthesised and fully characterised by a variety of spectroscopic and analytical techniques. The resultant complexes are luminescent in the orange region, revealing classical metal-to-ligand charge transfer ($^3$MLCT) ((Re (dπ) → (N^N^C)(π*)) emission in aerated DMSO solution. The red shifted emission observed on going from **3** to **4** suggests that the electronic properties of the gold ancillary ligand are implicated in the emissive properties. Antiproliferative activity in tumour cell lines, lung (A549) and cervix (HeLa) cells revealed that only complex **4** containing a 2,3,4,6-tetra-*O*-acetyl-1-thio-β-D-glucopyranose as gold ancillary ligand possesses certain cytotoxicity in both cell lines.

**KEYWORDS**
anticancer, gold, luminescence, rhenium

## 1 | INTRODUCTION

Heterometallic complexes are gaining increasing attention in many research fields, from catalysis[1] or material science[2] to medicine.[3] In the context of medical applications, many metallic combinations have been explored from merging two potential anticancer metallic fragments like $Fe^{II}$ with $Au^{I}$,[4] $Ru^{II}$ with $Pt^{II}$,[5] $Ti^{IV}$ with $Au^{I}$[6] or $Cu^{I}/Ag^{I}$ with $Au^{I}$[7] (Figure 1) or even not so obvious combination such as those associating emissive metallic fragments with antiproliferative ones. Examples of those are the mixtures of $d^6$ metal complexes with noble metals, which have been increasingly studied in the recent years; see Figure 1. In particular, complexes derived from $Re^{I}$ or $Ir^{III}$ combined with $Au^{I}$ species have been designed as theranostic agents, where the $d^6$ metallic core usually provides the emissive properties for cell imaging and the $Au^{I}$ fragment the therapeutics; see Figure 1.[8] It is well known that

Re(I) complexes of the type *fac*-[Re $(CO)_3$(diimime)X], where X represents a halogen, present phosphorescent emission due to a metal-to-ligand charge transfer ($^3$MLCT) transition involving the orbitals of the accepting diimine ligand.[9] As consequence of the forbidden nature of their emission, these types of complexes generally offer large Stokes' shifts and relatively long lifetimes, making them good candidates for bioimaging purposes.[10]

Alternatively, gold complexes have been used in the treatment of rheumatoid arthritis as anti-inflammatory drugs in the form of gold thiolates, as, for example, the disodium aurothiomalate salt or aurothioglucose, among others.[14] In addition, more recently, they have gained importance in the design of novel anticancer agents, especially since auranofin, initially used as an antiarthritic drug, had entered in four clinical trials, chronic lymphocytic leukaemia (NCT01419691 and NCT01747798), ovarian cancer (NCT03456700) and lung cancer (NCT01737502) treatment.[15] Many studies have demonstrated that a judicious ligand selection can deliver gold complexes with great antiproliferative activity against a wide range of different cancer cell lines.[16] In the search to optimise the anticancer activity of gold complexes, N-heterocyclic carbene (NHC) species have arisen as a new source of ligands with great prospects in medicine.[17] In fact, gold carbene bonds present a strong σ-donating ability, being comparable with that of phosphines, an essential component in the auranofin drug. In this sense, multidentate fused imidazole [4,5,f]-1,10-phenanthroline derivatives could be thought as a great ally to bring together a luminescent $Re^I$ fragment and a therapeutic $Au^I$ species. Coordination of the *fac*-{Re $(CO)_3$X} core to the phenanthroline unit will ensure to retain the typical emissive properties for $Re^I$ complexes, whereas the gold coordination to the further functionalised fussed imidazole will deliver a robust gold carbene derivative that can be easily tuned by further derivatisation of the gold ancillary ligand. On top of that, it cannot be overlooked that imidazo[4,5-f]-1,10-phenanthroline has a tremendous synthetic versatility. Functionalisation of imidazolyl nitrogens with residues such as morpholine,[18] aryl groups[19] or hydrocarbon chains[20] can be easily approached, delivering diverse photophysical and, in some cases, bioactive properties; see Figure 2.

In this paper, the synthesis of a series heterobimetallic $Re^I/Au^I$ coordinated through a fused imidazo [4,5-f]-1,10-phenanthroline core (N^N^C) is reported. The rhenium centre is bonded in a bidentate fashion to the two nitrogen atoms of the phenanthroline, whereas the gold metal binds to the carbene carbon of the fused imidazolium to deliver neutral complexes with a general formula of *fac*-[ReCl $(CO)_3$(N^N^CAuR)], being R an iodide, phenylacetylene, dodecanethiol and 2,3,4,6-tetra-*O*-acetyl-1-thio-β-D-glucopyranose. Moreover, two cationic complexes, a bimetallic *fac*-[ReCl $(CO)_3$(N^N^CAuJohnPhos)]$^+$ and a trimetallic [(*fac*-[ReCl $(CO)_3$(N^N^C)])$_2$Au]$^+$ species, are also described. Variation of the gold ancillary ligand is discussed in the

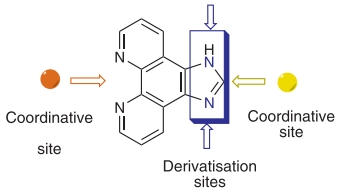


**FIGURE 2** Synthetic versatility offered by of imidazo[4,5-f]-1,10-phenanthroline (N^N) with potential tridentate (N^N^C) coordination

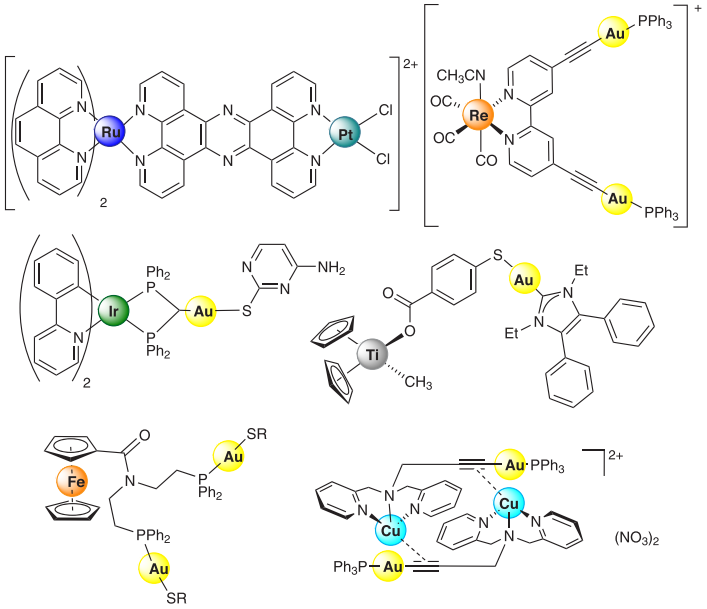

**FIGURE 1** Depiction of heterometallic $Ru^{II}/Pt^{II,11}$ $Re^I/Au^{I,12}$ $Ir^{III}/Au^{I13}$ $Ti^{IV}/Au^{I,5}$ $Fe^{II}/Au^{I4}$ and $Cu^I/Au^{I7}$ complexes

context of their photophysical and antiproliferative properties.

## 2 | RESULTS AND DISCUSSION

### 2.1 | Synthesis and characterisation

Following a similar approach to that described by J. O. Hoberg and collaborators,[21] the precursor Re(I) imidazolium salt (**D**) was isolated; see Scheme 1. In short, the synthesis began with the generation of imidazo [4,5-f]-1,10-phenanthroline (**A**) from the commercial available 1,10-phenanthroline-5,6-dione.[22] Thereafter, alkylation reaction was performed with iodopentane in basic conditions and subsequent coordination reaction to the rhenium pentacarbonyl chloride by displacement of two carbonyl ligands was successfully accomplished to afford (**C**). Finally, the imidazolium salt (**D**) was obtained after quaternisation of the imidazolyl nitrogen with methyl iodide. Heterobimetallic complex **1** was then prepared following a simple and efficient method described by our group for the generation of NHC gold(I) complexes.[23] The procedure entails a one-pot reaction using mild conditions, where (**D**) and [AuCl (tht)] were stirred in the presence of $NBu_4(acac)$ in a mixture of solvents to facilitate both, solubility of reagents and side products, as well as precipitation of the desired heterobimetallic complex **1**.

The disappearance of the imidazolyl proton at 10.06 ppm in $^1$H-NMR together with the shift observed for the aromatic protons upon coordination is indicative of the accomplishment of the reaction (see Figure 3). Moreover, $^{13}$C-NMR spectroscopy showed a peak downfield shifted to 188.9 ppm correspondent to the carbenic carbon. As a gold chloride complex, [AuCl (tht)], was used for the formation of **1**, there is the possibility that the chloride would remain directly bonded to the gold centre instead of a iodide. However, the lack of any band with in the FT-IR spectrum assigned to the υ (Au-C) at around 320 $cm^{-1}$ discard such possibility, pointing towards an iodide as the gold ancillary ligand.

Thereafter, complexes **2**–**4** were easily obtained from complex **1** by substitution of the iodide by the correspondent ancillary ligand, phenylacetylene, dodecanethiol and 2,3,4,6-tetra-*O*-acetyl-1-thio-β-D-glucopyranose, respectively, in the presence of a base; see Scheme 2.

All the complexes were successfully characterised by $^1$H, $^{13}$C{$^1$H} NMR spectroscopy, infrared spectroscopy and mass spectrometry. Characteristic shifts in $^1$H, $^{13}$C{$^1$H} NMR are observed for all the complexes corroborating the gold coordination to the desired ancillary ligand. Specifically, the alkynyl carbons suffer a shift to low field from 50 to 120 ppm upon coordination to the gold fragment in the case of complex **2**. Similarly, the characteristic shift seen by -C*H*$_2$S- protons from 2.50 to 3.01 ppm indicates the formation of complex **3**. In addition to these changes, also, the carbenic carbon shifted to low field upon the different gold functionalisation, going from 188.9 in complex **1** to 195.17 and 194.50 ppm for complexes **2** and **3**, respectively. In the case of complex **4**, confirmation of 2,3,4,6-tetra-*O*-acetyl-1-thio-β-D-glucopyranose coordination to the gold metal centre was evident after the appearance of signals for the two stereoisomers of **4** in $^1$H-NMR spectroscopy in a ration 1:1. It is important to notice that the lack of symmetry of complex **1** together with the stereogenic centres from the thiolate ligand delivers a stoichiometric mixture of diastereomers, distinguishable by $^1$H-NMR spectroscopy; see Figure 4.

Cationic complexes were then proposed to facilitate the cellular recognition and increase the possible antiproliferative effect against cancer cells. Thus, complexes **5** and **6** were synthesised, both from an analogous imidazolium salt to that of complex **D**, containing this time a noncoordinating counterion such as tetraphenyl borate; see Scheme 3. Complex **E** was also previously described in the literature by Hoberg and collaborators, and it was synthesised from **D** via a counterion metathesis reaction.[21] Thereafter, addition of complex **1** to a solution of **E** in the presence of $K_2CO_3$ rendered the desired biscarbene **5** in good yield (93%). Alternatively, addition of [AuCl (JohnPhos)] and $Bu_4N(acac)$ to complex **E** afforded complex **6**, which presented a single peak in $^{31}$P{$^1$H} NMR at 61.1 ppm corroborating the accomplishment of the reaction; see Figure S23. Once again, $^{13}$C-NMR spectroscopy showed peaks at 191.40 and 196.50 ppm corresponding to the carbenic carbon of **5** and **6**, respectively, revealing the strong

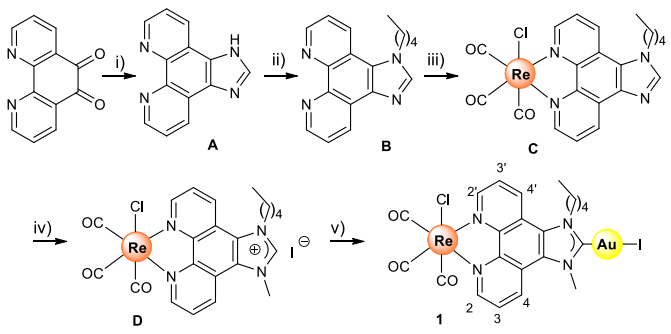


**SCHEME 1** (i) $NH_4OAc$, formaldehyde, acetic acid glacial, 110°C, 4 h; Addition $NH_3(aq)$ to pH 8–9; (96% yield); (ii) Iodopentane, NaOH, DMSO (59% yield); (iii) [$ReCO_5Cl$], toluene, 80°C, 12 h, (84% yield); (iv) MeI, DMF, 100°C, 3 days. (97% yield); (v) [AuCl (tht)], $NBu_4(acac)$, DCM:MeOH (2:1), 2.5 h, rt, (82% yield)

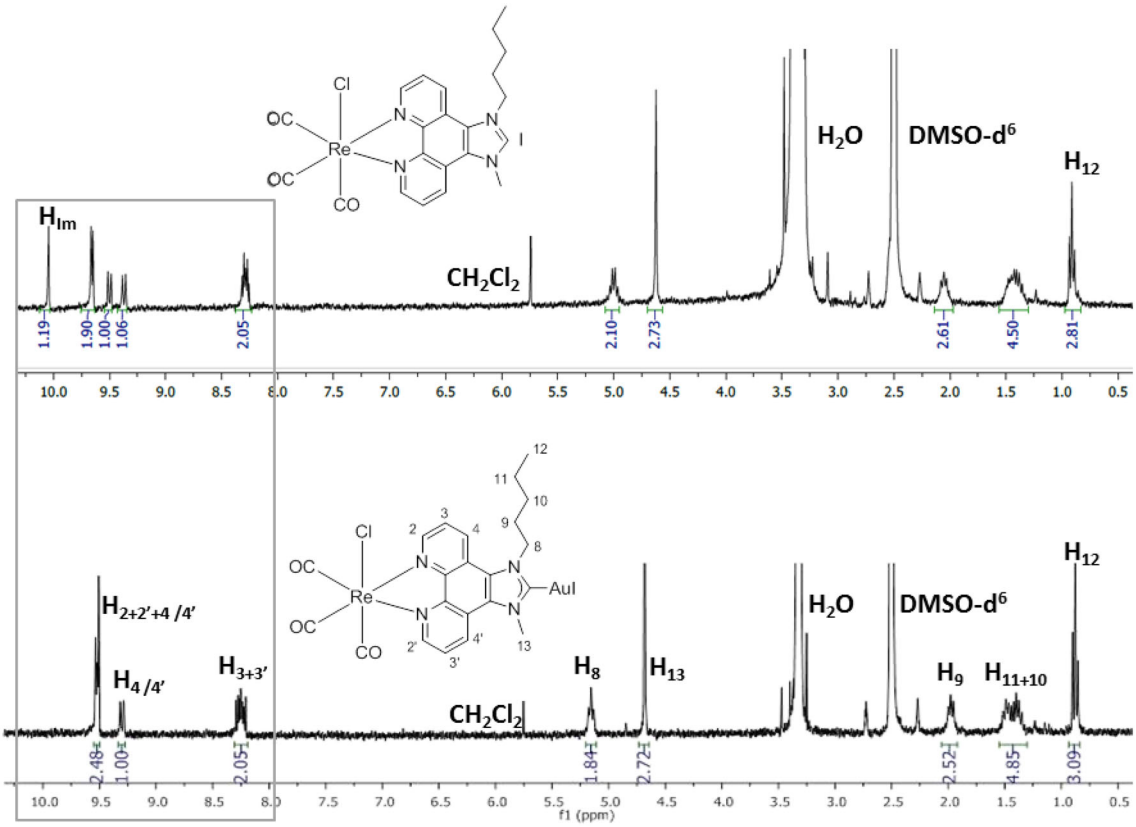


FIGURE 3 $^{1}$H-NMR spectra of complexes (**D**) and **1** in DMSO-$d_6$

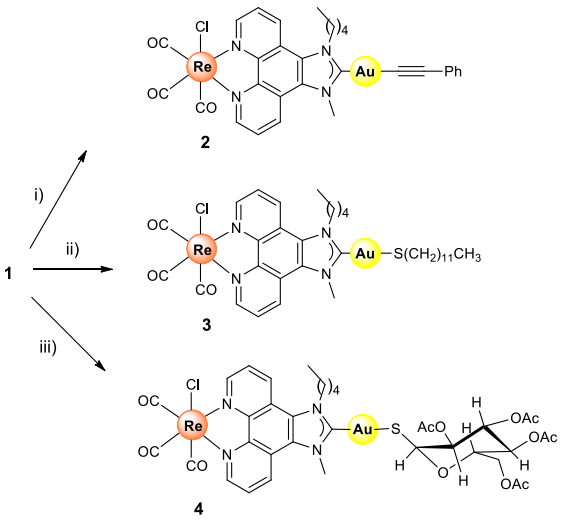


SCHEME 2 Synthesis of **2**–**4**. (i) Phenylacetylene, KOH, MeOH, rt, 12 h, 80% yield; (ii) dodecanethiol, $K_2CO_3$, DCM, rt, 12 h, 79% yield; (iii) 2,3,4,6-tetra-*O*-acetyl-1-thio-β-D-glucopyranose, $K_2CO_3$, DCM, rt, 12 h, 76% yield

electronic influence of the gold ancillary ligand into the chemical shifts observed. Therefore, carbonic carbon in **5** (*C* (NHC)-Au-*C* (NHC)) is more shielded in comparison with that of complex **6** (*C* (NHC)-Au-$PR_2R$). Such behaviour can be assignable to the existing π-back bonding between the metal and the phosphine that reduces the electronic contribution seen by the carbenic carbon in the case of complex **6**. The same effect is also observed for N-methyl protons; the closest protons to the metallic core, being those of complex **6,** are also deshielded in comparison with those of complex **5**.

On top of that, in all cases, the infrared spectrum presents two strong bands within the region 2020–1890 $cm^{-1}$ revealing the $C_{3v}$ symmetry of the complexes and in consequence the expected facial disposition of the carbonyl ligands. Specifically, the band at approximately 2020 $cm^{-1}$ corresponds to absorbance of the A′(1) mode, whereas the one at lower energy to the overlapping absorption of the A′(2) and A″ modes.[24]

## 2.2 | Photophysical studies

Since the complexes stock solution for the biological assays are prepared in DMSO, this solvent was chosen for the photophysical studies in order to have a good approximation to their photophysical behaviour in biological conditions. Therefore, photophysical properties of

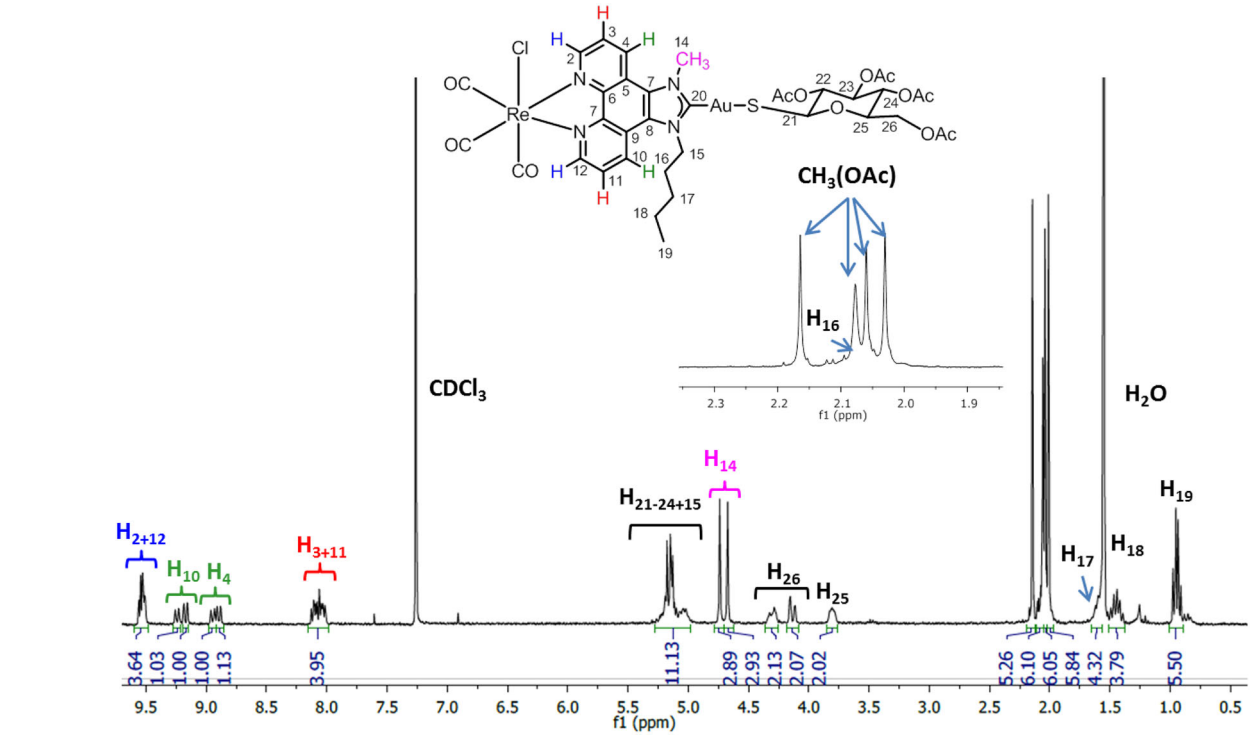


FIGURE 4 $^{1}$H-NMR spectrum of complex **4** in $CDCl_3$

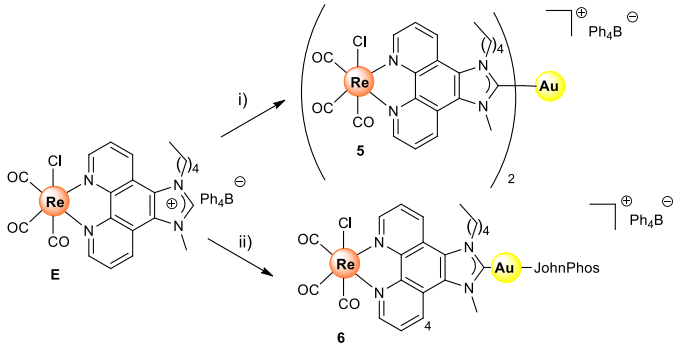


SCHEME 3 Synthesis of complexes **5** and **6.** (i) **1**, $K_2CO_3$, DCM, rt, 30 h, 93%; (ii) [AuCl (JohnPhos)], $NBu_4$(acac), DCM, rt, 12 h, 63%

complexes **1–6** were measured in aerated DMSO solution at room temperature. The most significant data are collected in Table 1 and Figure 5. By comparison with analogous complexes described in the literature,[25] absorption of the complexes **1–6** can be described as a combination of metal-perturbed ligand centred transitions (LC) at high energies, combined with metal to ligand (Re(d) → N^N^C (π*)) charge transfer transitions (MLCT) in the visible region. LC transitions are broad bands including π → π* and n → π* transitions mainly within the fused imidazo[4,5-f]-1,10-phenanthroline core (N^N^C). As expected, the extinction coefficients of the LC transitions are greater than those from the MLCT at approximately

TABLE 1 Absorption, emission and excitation maxima of complexes **1–6** measured in aerated DMSO at 298 K

| Complex | $^{1}$IL, $\lambda_{abs}$/nm ($\varepsilon \times 10^3$) | $^{1}$MLCT, $\lambda_{abs}$/nm ($\varepsilon \times 10^3$) | $\lambda_{exc}$ (λ/nm) | $\lambda_{em}$ (λ/nm) |
|---|---|---|---|---|
| 1 | 264 (59.8) | 398 (4.9) | 364, 451 | 650 |
| 2 | 280 (61.9) | 399 (5.1) | 362, 444 | 652 |
| 3 | 261 (35.7) | 402 (4.6) | 375, 406 | 652 |
| 4 | 262 (48.3), 291 (36.4) | 400 (5.4) | 369, 438 | 673 |
| 5 | 276 (92.7) | 395 (11.5) | 352, 470 | 641 |
| 6 | 263 (57.1) | 398 (5.1) | 362, 453 | 655 |

*Note*: ($\varepsilon$/dm$^3$mol$^{-1}$ cm$^{-1}$), Complex **D**, $\lambda_{em}$: 665 nm ($\lambda_{exc}$: 341, 470 nm).

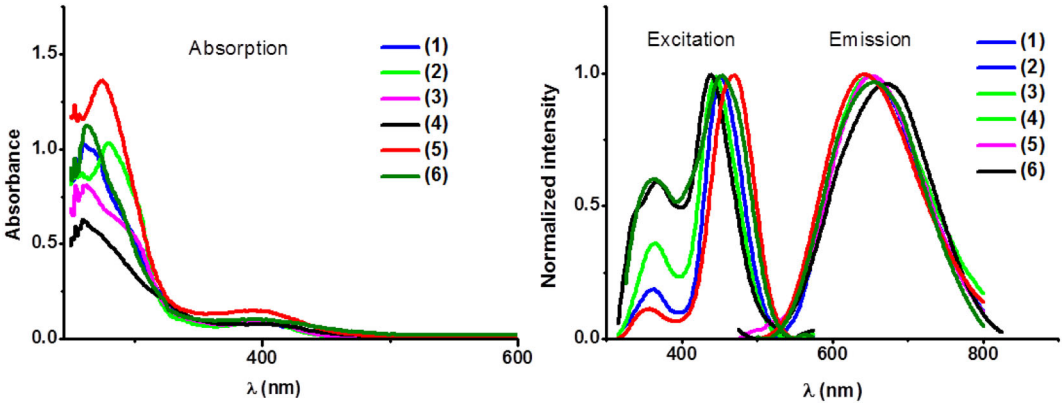


**FIGURE 5** Absorption (left) spectra and excitation and emission (right) spectra of complexes **1**–**6** recorded in DMSO at rt

**TABLE 2** $IC_{50}$ vales (μM) of complexes **1**–**6** incubated with A549 and HeLa cells incubated at 24 and 72 h

| Complex | A549 24 h | A549 72 h | HeLa 24 h | HeLa 72 h |
|---|---|---|---|---|
| 1 | >50 | >25 | - | >25 |
| 2 | >50 | >25 | >25 | >25 |
| 3 | >50 | >25 | - | >25 |
| 4 | >50 | 18.70 ± 4.67 | >25 | 22.9 ± 1.98 |
| 5 | >50 | >25 | >25 | >25 |
| 6 | >50 | >25 | >25 | >25 |

400 nm. Regarding the emissive properties, all complexes presented a broad and nonstructured emissive band between 641 and 673 nm, with Stokes' shifts over 200 nm that reveals the expected phosphorescence nature for this type of Re(I) complexes. Thus, such emission pattern can be assigned to a $^3$MLCT transition, which is consistent with the emissive behaviour observed for analogous Re(I) complexes of the general formula [ReCl$(CO)_3$(N^N)] reported in the literature.[26] As depicted in Table 1, the $^3$MLCT energy slightly varies to higher energies from 665 nm in the monometallic complex **D** to approximately 650 nm for the heterobimetallic complexes **1**–**3**, **5** and **6**, suggesting an energy gap increment within the frontier orbitals HOMO-LUMO (highest occupied molecular orbital - lowest unoccupied molecular orbital) of the heterobimetallic species. On the contrary, complex **4** containing the coordinated thiolate ligand displayed an emission maxima shifted to lower energies (675 nm) in comparison with the monometallic complex **D** and their analogous heterobimetallic counterparts. Such different emission, especially when the focus is set on complexes **3** and **4**, both containing a thiolate as the gold ancillary ligand, reveals that the challenging work of predicting the photophysical properties for this type of complexes, as not only electronic but also solvent and conformational properties, among other, could be involved.[27]

## 2.3 | Biological properties

The antiproliferative activity of complexes **1** to **6** was analysed by MTT assay in lung cancer A549 and cervix cancer HeLa cell lines to address their potential application as anticancer agents, see Table 2. The experiments were performed at different incubation times, 24 and 72 h, as it is known that alkynyl gold derivatives like complex **2** need longer times to reveal their cytotoxicity in comparison, for instance, with auranofin analogues (-SAuP-), probably because of a slower cellular uptake.[16,28] Such time delay for revealing the cytotoxiciy might be associated with the strength of gold-carbon bond in alkynyl gold complexes, which is one of the strongest gold-ligand bonds.[29] In the present case, none of the complexes showed antiproliferative activity below the studied concentration in A549 and HeLa cells at 24 h. Only complex **4** displayed certain cytotoxicity in both cell lines at longer times (72 h) $IC_{50} = 18.70 \pm 4.67$ μM (A549 cells) and 22.9 ± 1.98 μM (HeLa). This result emphasises

the importance of the optimum design of the gold coordination sphere. It is worth noticing that gold carbene bonds present a strong σ-donating ability, being comparable with that of phosphines. Therefore, from all the synthesised complexes, complex **4** is the one with the greatest structural similarity to that of commercially available drug auranofin, suggesting once again that probe design is the key step to deliver optimum anticancer agents.

$IC_{50}$ cisplatin (24 h, A549): 114.2 ± 9.1 μM,[30] (48 h, A549): 29.21 ± 1.92 μM,[31] (48 h, HeLa): 10.50 ± 1.51 μM.[31] $IC_{50}$ auranofin (24 h, A549): 7.59 μM,[32] (48 h, HeLa): 5.99 ± 0.01 μM.[33]

## 3 | CONCLUSIONS

In summary, six heterometallic $Re^I/Au^I$ complexes containing imidazo[4,5-f]-1,10-phenanthroline (N^N^C) as polytopic ligand were synthesised and their antiproliferative and emissive potential analysed. Specifically, four of them are neutral species following the formula *fac*-[Re $(CO)_3$Cl(N^N^C)AuR], where R is an iodide (**1**), phenylacetylene (**2**), dodecanethiol (**3**) or 2,3,4,6-tetra-*O*-acetyl-1-thio-β-D-glucopyranose (**4**), whereas the other two correspond to cationic species *fac*-[Re $(CO)_3$Cl (N^N^C)AuJohnPhos]$^+$ (**5**) and a trimetallic complex [(*fac*-[ReCl $(CO)_3$(N^N^C)])$_2$Au]$^+$ (**6**). Complexes **1** and **6** were prepared from the correspondent $Re^I$ imidazolium salt and subsequent reaction of **1** with the different R ligands in the presence of a base, delivered complexes **2**–**4** and **5**. The resultant complexes were orange emissive, revealing a classical $^3$MLCT ((Re (dπ) → N^N^C(π*)) emission. Despite the different gold ancillary ligand in complexes **1**–**6**, only complex **4** displayed a slightly red shifted emission in comparison with their analogues (675 vs. 650 nm) indicating that not only the electronic character of the ligands might be decisive for tuning the luminescence in this type of complexes. Analysis of the antiproliferative activity in lung cancer A549 cells and cervix HeLa cells showed that only complex **4** possesses certain cytotoxicity in both cell lines. These results suggest the importance of selecting the optimal gold coordinative ligands to deliver antiproliferative activity and ultimately gold-based drugs.

## 4 | EXPERIMENTAL

### 4.1 | Starting materials

The starting materials [AuCl (tht)],[34] [AuClPPh$_3$][35] and [Au (acac)PPh$_3$][36] were prepared according to published procedures. [Re $(CO)_5$Cl] and [$PdCl_2(PPh_3)_2$] were purchased from STREM Chemicals and TCI, respectively, and used as received. All other reagents were commercially available and were used without further purification. Solvents were dried with a SPS solvent purification system.

### 4.2 | Instrumentation

Mass spectra were recorded on a Bruker Esquire 3000 PLUS, with the electrospray ionization (ESI) technique and on a Bruker Microflex (MALDI-TOF). $^1$H, $^{13}$C{$^1$H} and $^{31}$P{$^1$H} were recorded at room temperature on a Bruker Avance 400 spectrometer ($^1$H 400.0, $^{13}$C 100.6 and $^{31}$P 162.0 MHz) or on a Bruker Avance II 300 spectrometer ($^1$H 300.0, $^{13}$C 75.5 and $^{31}$P 121.5 MHz) with chemical shifts (δ, ppm) reported relative to the solvent peaks of the deuterated solvent. All *J* values are given in Hz. IR spectra were recorded in neat samples on a Perkin-Elmer Spectrum 100FT-IR spectrometer. Room temperature steady-state emission and excitation spectra were recorded with a Jobin-Yvon-Horiba Fluorolog FL3-11 spectrometer fitted with a JY TBX picosecond detection module. UV–vis spectra were recorded with 1 cm quartz cells on an Evolution 600 spectrophotometer.

### 4.3 | Antiproliferative studies: MTT assay

Exponentially growing cells (A549 and HeLa) were seeded at a density of approximately $10^4$ cells per well in 96-well flat-bottomed microplates and allowed to attach for 24 h prior to addition of compounds. A stock solution of the complexes was prepared in DMSO 0.1 M. Subsequent dilutions of the different stock solutions from the complexes using DMEM were prepared. About 100 μl/well was added to the cells, in concentrations ranging from 0.5 to 50 μM containing as maximum 0.5% of DMSO. Each concentration was performed by quadruplicate. Cells were incubated with the complexes for either 24 h or 72 at 37°C. Thereafter, 10 μl of 3-(4,5-dimethylthiazol-2-yl)-2,5-diphenyltetrazolium bromide MTT (5 mg ml$^{-1}$) was added to each well and plates were incubated for further 2 h at 37°C. Finally, the growth media were eliminated and DMSO (100 μl per well) was added to dissolve the formazan precipitates. The optical density was measured at 550 nm using a 96-well multiscanner autoreader enzyme-linked immunosorbent assay (ELISA). The $IC_{50}$ values were calculated by nonlinear regression analysis.

## 4.4 | Synthesis

Numbering of complexes has been included in Figure S1 and reported spectra in Figures S2–S25.

### 4.4.1 | Synthesis of complex **1**

To a stirred solution of **D** (1 eq, 150 mg, 0.203 mmol) in a mixture of DCM (21 ml) and MeOH (14 ml) was added [AuCl (tht)] (1 eq, 65.1 mg, 0.203 mmol) followed by $NBu_4$(acac) (1 eq, 69.4 mg, 0.203 mmol). After 2.5 h in the dark, the yellow solution turned to a suspension. Solvent was evaporated to 1–2 ml, and more MeOH was added. The yellow solid was filtered and washed with MeOH (154.9 mg, 82%).

**$^1$H NMR (300 MHz, DMSO-$d_6$)**: δ 9.55–9.49 (m, 3H, $H_2 + H_{2'} + H_4$ or $H_{4'}$), 9.30 (d, $J = 8.6$ Hz, 1H, $H_4$ or $H_{4'}$), 8.27 (dd, $J = 8.7$, 5.1 Hz, 1H, $H_3$ or $H_{3'}$), 8.23 (dd, $J = 8.3$, 5.5 Hz, 1H, $H_3$ or $H_{3'}$), 5.15 (t, $J = 6.8$ Hz, 2H, $H_8$) 4.68 (s, 3H, $H_{13}$), 2.03–1.92 (m, 2H, $H_9$), 1.55–1.32 (m, 4H, $H_{10} + H_{11}$), 0.88 (t, $J = 7.1$ Hz, 3H, $H_{12}$). **$^{13}$C NMR (101 MHz, DMSO-$d_6$)**: δ 197.62 (s, CO), 188.67 (s, $C_{14}$), 152.96 (s, $C_2$ or $C_{2'}$), 152.87 (s, $C_2$ or $C_{2'}$), 144.48 (s, 2C, $C_6 + C_{6'}$), 134.28 (s, $C_4$ or $C_{4'}$), 133.75 (s, $C_4$ or $C_{4'}$), 127.33 (s, $C_3$ or $C_{3'}$), 127.05 (s, $C_{7'}$), 126.82 (s, $C_3$ or $C_{3'}$), 125.19 (s, $C_7$), 120.96 (s, $C_5$ or $C_{5'}$), 120.31 (s, $C_5$ or $C_{5'}$), 50.74 (s, $C_8$), 39.73 (s, $C_9$), 28.77 (s, $C_{13}$), 27.86 (s, $C_{10}$), 21.66 (s, $C_{11}$), 13.86 (s, $C_{12}$). **IR (cm$^{-1}$)**: 2016, 1885 υ (CO), 1,662 υ(N-C=O). Anal. calcd for $C_{22}H_{20}N_4O_3ClIReAu$: C, 28.29; H, 2.16; N, 6.00. Found: C, 28.16; H, 2.13; N, 5.90.

### 4.4.2 | Synthesis of complex **2**

To a solution of KOH (1.2 eq, 1.6 mg, 0.024 mmol) in MeOH (5 ml) was added **1** (1 eq, 20 mg, 0.021 mmol) and the resulting suspension was allowed to react overnight. Water was then added, and methanol was evaporated. DCM was added, and the organic phase was decantated and evaporated. The resulting solid was washed with MeOH to remove traces of water (15.2 mg, 80%).

**$^1$H NMR (400 MHz, DMSO-$d_6$)**: δ 9.53–9.49 (m, 3H, $H_2 + H_{2'} + H_4$ or $H_{4'}$), 9.27 (d, $J = 8.7$ Hz, 1H, $H_4$ or $H_{4'}$), 8.26 (dd, $J = 8.7$, 5.2 Hz, 1H, $H_3$ or $H_{3'}$), 8.21 (dd, $J = 8.6$, 5.2 Hz, 1H, $H_3$ or $H_{3'}$), 7.29–7.15 (m, 5H, $H_{Ar}$), 5.17 (t, $J = 7.1$ Hz, 2H, $H_8$), 4.70 (s, 3H, $H_{13}$), 2.04–1.93 (m, 2H, $H_9$), 1.57–1.47 (m, 2H, $H_{10}$), 1.44–1.35 (m, 2H, $H_{11}$), 0.90 (t, $J = 7.3$ Hz, 3H, $H_{12}$). **$^{13}$C NMR (101 MHz, DMSO-$d_6$)**: δ 197.62 (s, CO), 195.17 (s, $C_{14}$), 152.76 (s, $C_2$ or $C_{2'}$), 152.67 (s, $C_2$ or $C_{2'}$), 144.32 (s, $C_6 + C_{6'}$), 134.18 (s, $C_4$ or $C_{4'}$), 133.61 (s, $C_4$ or $C_{4'}$), 131.14 (s, 2C, $C_{19}$), 128.13 (s, $C_{18}$), 127.70 (s, $C_3$ or $C_{3'}$), 127.30 (s, $C_{17}$), 127.19 (s, $C_3$ or $C_{3'}$), 126.71 (s, $C_{20}$), 125.87 (s, $C_7$ or $C_{7'}$), 125.45 (s, $C_7$ or $C_{7'}$), 120.90 (s, $C_5$ or $C_{5'}$), 120.25 (s, $C_5$ or $C_{5'}$), 104.16 (s, $C_{16}$), 50.88 (s, $C_8$), 39.78 (s, $C_{13}$), 29.02 (s, $C_9$), 27.95 (s, $C_{10}$), 21.81 (s, $C_{11}$), 13.80 (s, $C_{12}$). **IR (cm$^{-1}$)**: 2018, 1890 υ (CO), 1,662 υ(N-C=O). **HRMS (m/z)**: 909.0857 $[M + H^+]$, $C_{30}H_{26}AuClN_4O_3Re$ (909.0916). Anal. calcd for $C_{30}H_{25}N_4O_3ClReAu{\cdot}H_2O$: C, 38.90; H, 2.94; N, 6.05. Found: C, 39.0; H, 3.04; N, 5.85.

### 4.4.3 | Synthesis of complex **3**

To a suspension of **1** (1 eq, 25 mg, 0.027 mmol) in degassed DCM (7 ml) was added dodecanethiol (1 eq, 4.9 µl, 0.025 mmol) followed by $K_2CO_3$ (excess). After 1 night of reaction, the suspension turned from yellow suspension to orange solution with remaining potassium carbonate. Water was then added, and the organic phase was decanted. The aqueous phase was extracted once with DCM, and then the combined organic phases were dried with anhydrous $Na_2SO_4$. DCM was concentrated, and hexane was added to afford an orange solid (21.5 mg, 79%).

**$^1$H NMR (400 MHz, $CDCl_3$)**: δ 9.50 (d, $J = 5.1$ Hz, 2H, $H_2 + H_{2'}$), 9.21 (d, $J = 8.6$ Hz, 1H), 8.90 (d, $J = 8.6$ Hz, 1H), 8.05 (dd, $J = 8.6$, 5.1 Hz, 1H, $H_3$ or $H_{3'}$), 8.03 (dd, $J = 8.6$, 5.1 Hz, 1H, $H_3$ or $H_{3'}$), 4.99 (t, $J = 7.2$ Hz, 2H, $H_8$), 4.63 (s, 3H, $H_{13}$), 3.01 (t, $J = 7.6$ Hz, 1H, $H_{15}$), 2.01–1.91 (m, 2H, $H_9$), 1.80 ($q_{ap}$, $J = 7.6$ Hz, 2H, $H_{16}$), 1.56–1.45 (m, 4H, $H_{10} + H_{17}$), 1.45–1.36 (m, 2H, $H_{11}$), 1.36–1.19 (m, 16H, $H_{18}$ to $H_{25}$), 0.92 (t, $J = 7.2$ Hz, 3H, $H_{12}$), 0.87 (d, $J = 6.9$ Hz, 3H, $H_{26}$). **$^{13}$C NMR (101 MHz, $CDCl_3$)**: δ 196.79 (s, CO), 194.50 (s, $C_{14}$), 188.75(?), 152.78 (s, $C_2$ or $C_{2'}$), 152.64 (s, $C_2$ or $C_{2'}$), 145.57 (s, $C_6$ or $C_{6'}$), 145.51 (s, $C_6$ or $C_{6'}$), 131.79 (s, $C_4$ or $C_{4'}$), 131.74 (s, $C_4$ or $C_{4'}$), 127.08 (s, $C_7$), 126.82 (s, $C_3$ or $C_{3'}$), 126.73 (s, $C_3$ or $C_{3'}$), 125.82 (s, $C_{7'}$), 121.18(s, $C_5$ or $C_{5'}$), 120.69 (s, $C_5$ or $C_{5'}$), 51.89 (s, $C_8$), 40.33 (s, $C_{13}$), 38.76 (s, $C_{16}$), 32.08 (s, $C_{alk}$), 29.91 (s, $C_{alk}$), 29.89 (s, $C_{alk}$), 29.83 (s, $C_{alk}$), 29.74 (s, $C_{alk}$), 29.70 (s, $C_{alk}$), 29.52 (s, $C_{alk}$), 28.75 (s, $C_{alk}$), 28.59 (s, $C_{alk}$), 22.84 (s, $C_{alk}$), 22.48 (s, $C_{alk}$), 14.28 (s, $C_{26}$), 14.01 (s, $C_{26}$). **IR (cm$^{-1}$)**: 2019, 1893 υ (CO), 1,662 υ(N-C=O). Anal. calcd for $C_{34}H_{45}N_4O_3ClReAuS{\cdot}2CH_2Cl_2$: C, 36.70; H, 4.19; N, 4.75; S, 2.72 Found: C, 36.97; H, 4.27; N, 5.35 S, 3.00.

### 4.4.4 | Synthesis of complex **4**

To a suspension of **1** (1 eq, 60 mg, 0.064 mmol) in DCM (10 ml) was added 2,3,4,6-tetra-*O*-acetyl-1-thio-

β-D-glucopyranose (1 eq, 26.5 mg, 0.070 mmol) followed by $K_2CO_3$ in excess. After 1 night of reaction, the suspension turned from yellow suspension to orange solution with remaining potassium carbonate. The suspension was filtered over celite, and the filtrate was concentrated and purified by silica gel column chromatography employing 97/3 DCM/MeOH as eluent (57.1 mg, 76%).

**$^1$H NMR (300 MHz, $CDCl_3$)**: δ 9.59–9.51 (m, 4H, $H_{2-+}H_{2'} + H_{12} + H_{12'}$), 9.26 (d, $J = 8.7$ Hz, 2H, $H_{10}$ or $H_{10'}$), 9.22–9.15 (d, $J = 8.5$ Hz, 2H, $H_{10}$ or $H_{10'}$), 8.97 (d, $J = 9.0$ Hz, 2H, $H_4$ or $H_{4'}$), 8.91 (d, $J = 8.7$ Hz, 2H, $H_4$ or $H_{4'}$), 8.16–8.02 (m, 4H, $H_{3+}H_{3'} + H_{11} + H_{11'}$), 5.29–4.97 (m, 12H, $H_{21-24} + H_{21'-24'} + H_{15} + H_{15'}$), 4.76 (s, 3H, $H_{14}$), 4.69 (s, 3H, $H_{14'}$), 4.38–4.28 (m, 2H, $H_{26}$ or $H_{26'}$), 4.19–4.12 (m, 2H, $H_{26}$ or $H_{26'}$), 3.87–3.79 (m, 2H, $H_{25} + H_{25'}$), 2.16 (s, 6H, $CH_3$(OAc)), 2.13–2.01 (m, 4H, $H_{16} + H_{16'}$), 2.08 (s, 6H, $CH_3$(OAc)), 2.06 (s, 6H, $CH_3$(OAc)), 2.03 (s, 6H, $CH_3$(OAc)), 1.67–1.56 (m, 4H, $H_{17} + H_{17'}$), 1.46 (dt, $J = 14.5$, 7.4 Hz, 4H, $H_{18} + H_{18'}$), 0.97 (td, $J = 7.4$, 5.5 Hz, 6H, $H_{19} + H_{19'}$). **$^{13}$C NMR (101 MHz, $CDCl_3$)**: δ 196.78 (s, C ≡ O), 196.77 (s, C ≡ O), 196.75 (s, C ≡ O), 196.71 (s, C ≡ O), 188.75 (s, C ≡ O), 188.73 (s, C ≡ O), 170.85 (s, C=O), 170.32 (s, C=O), 170.22 (s, C=O), 169.97 (s, C=O), 153.05 (s, $C_2$ or $C_{2'}$ or $C_{12}$ or $C_{12'}$), 152.80 (s, 2C, $C_2$ or $C_{2'}$ or $C_{12}$ or $C_{12'} + C_2$ or $C_{2'}$ or $C_{12}$ or $C_{12'}$), 152.62 (s, $C_2$ or $C_{2'}$ or $C_{12}$ or $C_{12'}$), 145.60 (s, $C_6$ or $C_{6'}$ or $C_{13}$ or $C_{13'}$), 145.58 (s, $C_6$ or $C_{6'}$ or $C_{13}$ or $C_{13'}$), 145.53 (s, $C_6$ or $C_{6'}$ or $C_{13}$ or $C_{13'}$), 145.35 (s, $C_6$ or $C_{6'}$ or $C_{13}$ or $C_{13'}$), 131.90 (s, 2C, $C_4$ or $C_{4'}$ or $C_{10}$ or $C_{10'} + C_4$ or $C_{4'}$ or $C_{10}$ or $C_{10'}$), 131.81 (s, $C_4$ or $C_{4'}$ or $C_{10}$ or $C_{10'}$), 131.75 (s, $C_4$ or $C_{4'}$ or $C_{10}$ or $C_{10'}$), 127.06 (s, $C_8$ or $C_{8'}$), 127.03 (s, $C_8$ or $C_{8'}$), 126.90 (s, 2C, $C_3$ or $C_{3'}$ or $C_{11}$ or $C_{11'} + C_3$ or $C_{3'}$ or $C_{11}$ or $C_{11'}$), 126.85 (s, $C_3$ or $C_{3'}$ or $C_{11}$ or $C_{11'}$), 126.74 (s, $C_3$ or $C_{3'}$ or $C_{11}$ or $C_{11'}$), 125.84 (s, $C_7$ or $C_{7'}$), 125.69 (s, $C_7$ or $C_{7'}$), 121.17 (s, $C_5$ or $C_{5'}$), 121.12 (s, $C_5$ or $C_{5'}$), 120.76 (s, $C_9$ or $C_{9'}$), 120.56 (s, $C_9$ or $C_{9'}$), 83.32 (s, $C_{21} + C_{21'}$), 78.18 (s, $C_{22}$ or $C_{23}$ or $C_{24}$), 76.09 (s, $C_{25} + C_{25'}$), 74.42 (s, $C_{22}$ or $C_{23}$ or $C_{24}$), 69.15 (s, $C_{22}$ or $C_{23}$ or $C_{24}$), 63.07 (s, $C_{26} + C_{26'}$), 51.97 (s, $C_{15}$ or $C_{15'}$), 51.73 (s, $C_{15}$ or $C_{15'}$), 40.47 (s, $C_{14}$ or $C_{14'}$), 40.27 (s, $C_{14}$ or $C_{14'}$), 31.06 (s, 2C, $CH_3OAc$), 29.75 (s, $C_{16}$ or $C_{16'}$), 29.63 (s, $C_{16}$ or $C_{16'}$), 28.66 (s, $C_{17}$ or $C_{17'}$), 28.55 (s, $C_{17}$ or $C_{17'}$), 22.79 (s, $C_{18}$ or $C_{18'}$), 22.49 (s, $C_{18}$ or $C_{18'}$), 22.46 (s), 21.41 (s, 2C, $CH_3OAc$), 20.87 (s, 2C, $CH_3OAc$), 20.82 (s, 2C, $CH_3OAc$), 13.97 (s, $C_{19}$ or $C_{19'}$), 13.93 (s, $C_{19}$ or $C_{19'}$). **IR ($cm^{-1}$)**: 2020, 1890 υ (CO), 1746 υ(O-C=O), 1,220, 1,032 υ(C-O st). **HRMS (m/z)**: 1193.1075 [M + Na], $C_{36}H_{39}AuClN_4O_{12}ReS$ (1193.1080). Anal. calcd for $C_{36}H_{39}N_4O_8ClReAuS{\cdot}4CH_2Cl_2$: C, 33.22; H, 3.28; N, 3.87; S, 2.22 Found: C, 33.12; H, 3.01; N, 4.28 S, 2.27.

### 4.4.5 | Synthesis of complex **5**

To a suspension of **E** (1 eq, 20 mg, 0.0215 mmol) in DCM (7 ml) was added **1** (1 eq, 20.1 mg, 0.0215 mmol) followed by excess of potassium carbonate. After 31 h at r.t., water was added and the organic layer was decanted. The aqueous phase was washed with DCM (2 × 10 ml), and the combined organic phases were dried with anhydrous sodium sulphate. The suspension was decanted from the sodium sulphate, and the solvent evaporated. After dissolving in acetone and filtration over celite, addition of petroleum ether afforded a yellow-orange solid (34.5 mg, 93%).

**$^1$H NMR (400 MHz, DMSO-$d_6$)**: δ 9.65–9.54 (m, 6H, $H_2 + H_{2'} + H_3$ or $H_{3'}$), 9.40–9.33 (m, 2H, $H_3$ or $H_{3'}$), 8.29 (d, $J = 5.2$ Hz, 4H, $H_4 + H_{4'}$), 7.20–7.14 (t, $J = 7.4$ Hz, 8H, $H_{meta}$), 6.94–6.91 (t, $J = 7.4$ Hz, 8H, $H_{ortho}$), 6.80–6.75 (t, 4H, $H_{para}$), 5.30 ($s_{br}$, 4H, $H_8$), 4.84 (s, 6H, $H_{13}$), 2.13–2.06 (m, 4H, $H_9$), 1.64–1.56 (m, 4H, $H_{10}$), 1.46–1.34 (m, 4H, $H_{11}$), 0.90 (t, $J = 7.3$ Hz, 4H, $H_{12}$). **$^{13}$C NMR (101 MHz, DMSO-$d_6$)**: δ 197.59 (s, CO), 196.51 (s, CO), 191.40 (s, 1C, $C_{14}$), 191.35 (s, 1C, $C_{14'}$), 189.73 (s, CO), 188.55 (s, CO), 163.34 (q, $^1J_{P-B} = 49.4$ Hz, 4C, *ipso*-C, $BPh_4$), 153.33 (s, 4C, $C_2 + C_{2'}$), 144.64 (s, 4C, $C_6 + C_{6'}$), 135.51 ($s_{br}$, 8C, *meta*-C, $BPh_4$), 134.23 (s, 2C, $C_3$ or $C_{3'}$), 133.59 (s, 2C, $C_3$ or $C_{3'}$), 127.62 (s, 2C, $C_7$ or $C_{7'}$), 127.41 (s, 2C, $C_4$ or $C_{4'}$), 126.67 (s, 2C, $C_4$ or $C_{4'}$), 125.80 (s, 2C, $C_7$ or $C_{7'}$), 125.27 (q, $^2J_{P-B} = 2.7$ Hz, 8C, *ortho*-C, $BPh_4$), 121.49 ($s_{br}$, 4C, *para*-C, $BPh_4$), 120.96 (s, 2C, $C_5$ or $C_{5'}$), 120.34 (s, 2C, $C_5$ or $C_{5'}$), 51.50 (s, 2C, $C_8 + C_{8'}$), 39.91 (s, 2C, $C_{13} + C_{13'}$), 29.37 (s, 2C, $C_9 + C_{9'}$), 28.37 (s, 2C, $C_{10} + C_{10'}$), 21.95 (s, 2C, $C_{11} + C_{11'}$), 13.85 (s, 2C, $C_{12} + C_{12'}$). **IR ($cm^{-1}$)**: 3057 υ ($C_{Ar}$-H) 2017, 1885 υ (CO). **HRMS (m/z)**: 1417.1189 $M^+$, $C_{44}H_{40}AuCl_2N_8O_6Re_2$ (1417.1218).

### 4.4.6 | Synthesis of complex **6**

To a stirred solution of **E** (1 eq, 60 mg, 0.0645 mmol) in DCM (5 ml) was added [AuCl (JohnPhos)] (1 eq, 34.2 mg, 0.0645 mmol) followed by $NBu_4$(acac) (1 eq, 22 mg, 0.0645 mmol). The reaction mixture was stirred 1 night at r.t. and evaporated. The crude was then washed several times with MeOH and finally recrystallised in $CH_3CN$/ether. (63.3 mg, 69%).

**$^1$H NMR (400 MHz, $CD_3CN$)**: δ 9.59 (dd, $J = 5.2$, 1.1 Hz, 1H, $H_2$ or $H_{2'}$), 9.58 (dd, $J = 5.1$, 1.1 Hz, 1H, $H_2$ or $H_{2'}$), 9.34 (dd, $J = 8.7$, 1.1 Hz, 1H, $H_3$ or $H_{3'}$), 9.04 (dd, $J = 8.7$, 1.1 Hz, 1H, $H_3$ or $H_{3'}$), 8.14 (dd, $J = 8.7$, 5.2 Hz, 1H, $H_4$ or $H_{4'}$), 8.11 (dd, $J = 8.7$, 5.2 Hz, 1H, $H_4$ or $H_{4'}$), 8.11–8.06 (m, 1H, $H_{JohnPhos}$), 7.68–7.63 (m, 2H,

$H_{JohnPhos}$), 7.38–7.30 (m, 6H, $H_{JohnPhos}$), 7.29–7.24 (m, 8H, $H_{ortho}$), 7.02–6.96 (m, 8H, $H_{meta}$), 6.86–6.81 (m, 4H, $H_{para}$), 4.79–4.73 (m, 2H, $H_8 + H_{8'}$), 4.39 (s, 3H, $H_{13}$),1.94–1.83 (m, 2H, $H_9 + H_{9'}$), 1.56–1.42 (m, 1H, $H_{10}$ or $H_{10'}$), 1.55 (s, 9H, $H_{28}$ or $H_{28'}$), 1.51 (s, 9H, $H_{28}$ or $H_{28'}$) 1.39–1.28 (m, 3H, $H_{10}$ or $H_{10'} + H_{11} + H_{11'}$), 0.87 (t, $J = 7.2$ Hz, 3H, $H_{12}$). **$^{31}$P NMR (162 MHz, $CD_2Cl_2$)**: δ 63.97 (s). **$^{13}$C NMR (101 MHz, DMSO-$d_6$)**: δ 196.50 (s, $C_{14}$), 196.19 (s, CO), 195.08 (s, CO), 188.53 (s, CO), 163.35 (q, $^1J_{P-B} = 49.3$ Hz, 4C, *ipso*-C, $BPh_4$), 153.44 (s, $C_2$ or $C_{2'}$), 153.35 (s, $C_2$ or $C_{2'}$), 148.70 (d, $^1J_{P-C} = 14.1$ Hz, $C_{15}$), 144.64 (s, 2C, $C_6 + C_{6'}$), 144.61 (s, 2C, $C_6 + C_{6'}$), 143.01 (d, $J^2 = 6.1$ Hz, $C_{20}$), 135.51 (s, 8C, *meta*-C, $BPh_4$), 134.75 (s, $C_{JohnPhos}$), 134.09 (s, $C_3$ or $C_{3'}$), 133.47 (s, $C_3$ or $C_{3'}$), 132.61 (d, $^2J_{P-C} = 7.7$ Hz, $C_{16}$), 131.33 (s, $C_{JohnPhos}$), 129.21–128.88 (m, 6C, $C_{JohnPhos}$), 127.87 (d, $^3J_{P-C} = 6.3$ Hz, $C_{17}$), 127.22 (s, $C_{4'}$), 127.11 (s, $C_5$ or $C_{5'}$), 126.66 (s, $C_4$), 125.58 (s, $C_5$ or $C_{5'}$), 125.26 (q, $^2J_{P-B} = 2.7$ Hz, 8C, *ortho*-C, $BPh_4$), 124.78 (s, $C_{21}$), 121.48 (s, 4C, *para*-C, $BPh_4$), 120.93 (s, $C_7$ or $C_{7'}$), 120.31 (s, $C_7$ or $C_{7'}$), 51.37 (s, $C_8$), 39.78 (s, $C_{13}$), 37.36 (d, $^1J_{P-C} = 23.4$ Hz, 2C, $C_{27}$), 30.49 (d, $^2J_{P-C} = 6.3$ Hz, 6C, $C_{28}$), 29.43 (s, $C_9$), 28.32 (s, $C_{11}$), 13.81 (s, $C_{12}$). **IR ($cm^{-1}$)**: 3053 υ ($C_{Ar}$-H) 2017, 1922, 1887 υ (CO). **HRMS (m/z)**: 1105.2256 $M^+$, $C_{42}H_{47}AuClN_4O_3Re$ (1105.2285). Anal. calcd for $C_{62}H_{67}N_4O_3ClReAuPB{\cdot}2CH_2Cl_2$: C, 49.70; H, 4.63; N, 3.62. Found: C, 50.55; H, 4.70; N, 3.69.

## ACKNOWLEDGEMENTS

Authors thank the Agencia Estatal de Investigación, projects PID2019-104379RB-C21/AEI /10.13039/501100011033, RTI2018-097836-J-I00/MCIN/AEI/10.13039/501100011033/FEDER, RYC2018-025872-I (funded by MCIN/AEI/10.13039/501100011033 and by "ESF Investing in your future"), RED2018-102471-T/MCIN/AEI/10.13039/501100011033, and Gobierno de Aragón-Fondo Social Europeo (E07_20R) for financial support. A.L. thanks the Gobierno de Aragón for a predoctoral fellowship.

## AUTHOR CONTRIBUTIONS

**Andrés Luengo:** Investigation; methodology. **Isabel Marzo:** Data curation; resources; visualization. **Vanesa Fernández-Moreira:** Conceptualization; formal analysis; funding acquisition; supervision; visualization. **Concepcion Gimeno:** Conceptualization; formal analysis; funding acquisition; project administration; resources; supervision.

## DATA AVAILABILITY STATEMENT

The data of this manuscript are available from the corresponding authors upon request.

## ORCID

*Andrés Luengo* https://orcid.org/0000-0002-0557-4631
*Isabel Marzo* https://orcid.org/0000-0002-2315-9079
*Vanesa Fernández-Moreira* https://orcid.org/0000-0002-1218-7218
*M. Concepción Gimeno* https://orcid.org/0000-0003-0553-0695

## REFERENCES

[1] J. A. Mata, F. E. Hahn, E. Peris, *Chem. Sci.* **2014**, *5*, 1723.
[2] M. Hardy, A. Lützen, *Chem. A Eur. J.* **2020**, *26*, 13332.
[3] M. Redrado, V. Fernández-Moreira, M. C. Gimeno, *ChemMedChem* **2021**, *16*, 932.
[4] H. Goitia, Y. Nieto, M. D. Villacampa, C. Kasper, A. Laguna, M. C. Gimeno, *Organometallics* **2013**, *32*, 6069.
[5] A. Jain, *Coord. Chem. Rev.* **2019**, *401*, 213067.
[6] N. Curado, N. Giménez, K. Miachin, M. Aliaga-Lavrijsen, M. A. Cornejo, A. A. Jarzecki, M. Contel, *ChemMedChem* **2019**, *14*, 1086.
[7] A. Johnson, I. Marzo, M. C. Gimeno, *Dalton Trans.* **2020**, *49*, 11736.
[8] V. Fernández-Moreira, M. C. Gimeno, *Chem. A Eur. J.* **2018**, *24*, 3345.
[9] D. R. Striplin, G. A. Crosby, *Chem. Phys. Letters* **1994**, *221*, 426.
[10] V. Fernández-Moreira, F. L. Thorp-Greenwood, M. P. Coogan, *Chem. Commun.* **2010**, *46*, 186.
[11] P. J. Jarman, F. Noakes, S. Fairbanks, K. Smitten, I. K. Griffiths, H. K. Saeed, J. A. Thomas, C. Smythe, *J. Am. Chem. Soc.* **2019**, *141*, 2925.
[12] A. Luengo, M. Redrado, I. Marzo, V. Fernández-Moreira, M. C. Gimeno, *Inorg. Chem* **2020**, *59*, 8960.
[13] M. Redrado, A. Benedi, I. Marzo, A. L. García-Otín, V. Fernández-Moreira, M. C. Gimeno, *Chem. A Eur. J.* **2021**, *27*, 9885.
[14] a) P. J. Sadler, *Gold Bull.* **1976**, *9*, 110; b) T. Zou, C. T. Lum, C.-N. Lok, J.-J. Zhang, C.-M. Che, *Chem. Soc. Rev.* **2015**, *44*, 8786.
[15] a) U.S. National Library of Medicine. Available from: https://clinicaltrials.gov; b) L. F. Boullosa, J. V. Loenhout, T. Flieswasser, J. De Waele, C. Hermans, H. Lambrechts, B. Cuypers, K. Laukens, E. Bartholomeus, V. Siozopoulou, W. H. De Vos, M. Peeters, E. L. J. Smits, C. Deben, *Redox Biol.* **2021**, *42*, 101949.
[16] V. Fernández-Moreira, R. P. Herrera, M. C. Gimeno, *Pure Appl. Chem.* **2019**, *91*, 247.
[17] M. Mora, M. C. Gimeno, R. Visbal, *Chem. Soc. Rev.* **2019**, *48*, 447.
[18] J.-B. Liu, K. Vellaisamy, G. Li, C. Yang, S.-Y. Wong, C.-H. Leung, S.-Z. Pu, D.-L. Ma, *J. Mater. Chem. B* **2018**, *6*, 3855.
[19] R. O. Bonello, M. B. Pitak, S. J. Coles, A. J. Hallett, I. A. Fallis, S. J. A. Pope, *J. Organomet. Chem.* **2017**, *841*, 39.
[20] L. Yingkui, *J. Lumin.* **2011**, *131*, 1599.
[21] A. A. Webster, S. K. K. Prasad, J. M. Hodgkiss, J. O. Hoberg, *Dalton Trans.* **2015**, *44*, 3728.
[22] J.-Z. Wu, B.-H. Ye, L. Wang, L.-N. Ji, J.-Y. Zhou, R.-H. Li, Z.-Y. Zhou, *J. Chem. Soc. Dalton Trans.* **1997**, 1395.
[23] A. Johnson, M. C. Gimeno, *Chem. Commun.* **2016**, *52*, 9664.

[24] a) D. M. Dattelbaum, K. M. Omberg, J. R. Schoonover, R. L. Martin, T. J. Meyer, *Inorg. Chem.* **2002**, *41*, 6071; b) I. Veroni, C. A. Mitsopoulou, F. J. Lahoz, *J. Organomet. Chem.* **2008**, *693*, 2451.

[25] R. O. Bonello, I. R. Morgan, B. R. Yeo, L. E. J. Jones, B. M. Kariuki, I. A. Fallis, S. J. A. Pope, *J. Organomet. Chem.* **2014**, *749*, 150.

[26] a) M. Wrighton, D. L. Morse, *J. Am. Chem. Soc.* **1974**, *96*, 998; b) L. A. Sacksteder, A. P. Zipp, E. A. Brown, J. Streich, J. N. Demas, B. A. DeGraff, *Inorg. Chem.* **1990**, (29), 4335.

[27] a) A. Kumar, S. S. Sun, A. J. Lees, Photophysics and photochemistry of organometallic rhenium diimine complexes, in *Photophysics of Organometallics. Topics in Organometallic Chemistry*, (Ed: A. Lees) Vol. 29, Springer, Berlin, Heidelberg **2009**; b) M. P. Coogan, V. Fernández-Moreira, J. B. Hess, S. J. A. Pope, C. Williams, *New J. Chem.* **2009**, *33*(33), 1094.

[28] a) L. Ortego, F. Cardoso, S. Martins, M. F. Fillat, A. Laguna, M. Meireles, M. D. Villacampa, M. C. Gimeno, *J. Inorg. Biochem.* **2014**, *130*, 32; b) A. Gutiérrez, C. Cativiela, A. Laguna, M. C. Gimeno, *Dalton Trans.* **2016**, *45*, 13483.

[29] a) H.-T. Liu, X.-G. Xiong, P.-D. Dau, Y.-L. Wang, D.-L. Huang, J. Li, L.-S. Wang, *Nat. Commun.* **2013**, *4*, 2223; b) E. Cerrada, V. Fernández-Moreira, M. C. Gimeno, *Adv. Organom. Chem.* **2019**, *71*, 227.

[30] M. Frik, J. Fernández-Gallardo, O. Gonzalo, V. Mangas-Sanjuan, M. González-Alvarez, A. Serrano Del Valle, C. Hu, I. González-Alvarez, M. Bermejo, I. Marzo, M. Contel, *J. Med. Chem.* **2015**, *58*, 5825.

[31] C. Marzano, V. Gandin, M. Pellei, D. Colavito, G. Papini, G. G. Lobbia, E. D. Giudice, M. Porchia, F. Tisato, C. Santini, *J. Med. Chem.* **2008**, *51*, 798.

[32] E. Hatem, S. Azzi, N. El Banna, T. He, A. Heneman-Masurel, L. Vernis, D. Baïlle, V. Masson, F. Dingli, D. Loew, B. Azzarone, P. Eid, G. Baldacci, M. Er-Huang, *J. Natl. Cancer Inst.* **2019**, *111*, 597.

[33] L. Ortego, F. Cardoso, S. Martins, M. F. Fillat, A. Laguna, M. Meireles, M. D. Villacampa, M. C. Gimeno, *J. Inorg. Biochem.* **2014**, *130*, 32.

[34] a) R. Usón, A. Laguna, M. Laguna, D. A. Briggs, H. H. Murray, J. P. Fackler Jr., Chapter 17 -(Tetrahydrothiophene)Gold(I) or Gold(III) Complexes, in *Inorganic Syntheses*, (Ed: H. D. Kaesz) Vol. 26, John Wiley & Sons, Inc, New York **1989** 85; b) G. Brauer, *Handbuch der Präparativen Anorganischen Chemie*, Ferdinand Enke Verlag, Stuttgart **1978** 1014.

[35] L. K. Batchelor, E. Paunescu, M. Soudani, R. Scopelliti, P. J. Dyson, *Inorg. Chem* **2017**, *56*, 9617.

[36] D. Gibson, B. F. G. Johnson, J. Lewis, *J. Chem. Soc. A* **1970**, 1730.

## SUPPORTING INFORMATION

Additional supporting information may be found in the online version of the article at the publisher's website.

**How to cite this article:** A. Luengo, I. Marzo, V. Fernández-Moreira, M. C. Gimeno, *Appl Organomet Chem* **2022**, e6661. https://doi.org/10.1002/aoc.6661